Deep Quantitative Proteomics Identifies Conserved Proteome Alterations in Low and High-Grade Serous Ovarian Cancers

Christopher M. Tarney[1,2*], Paulette Mhawech-Fauceglia[1], Jonathan Ogata[1,3], Julie Oliver[1,3], Tamara Abulez[1,3], Brian L. Hood[1,3], Kelly A. Conrads[1,3], Kendal Rosalik[4], Kwong-Kwok Wong[5], David M. Gershenson[5], Sanghoon Lee[5], Anil K. Sood[5], Robert C. Bast, Jr[6], Kathleen M. Darcy[1-3], Neil T. Phippen[1,2], G. Larry Maxwell[1,2,7], Thomas P. Conrads[1,2, 7], Nicholas W. Bateman[1-3*]

[1]Gynecologic Cancer Center of Excellence, Department of Gynecologic Surgery and Obstetrics, Uniformed Services University and Walter Reed National Military Medical Center, Bethesda, MD 20889, USA.

[2]The John P. Murtha Cancer Center, Uniformed Services University and Walter Reed National Military Medical Center, MD 20889, USA

[3]Henry M. Jackson Foundation for the Advancement of Military Medicine, Inc. Bethesda, MD 20817, USA.

[4]Department of Gynecologic Surgery and Obstetrics, Madigan Army Medical Center, Joint Base Lewis-McChord, WA 98431, USA.

[5]Department of Gynecologic Oncology and Reproductive Medicine, The University of Texas MD Anderson Cancer Center, Houston, TX 77030, USA.

[6]Department of Experimental Therapeutics, The University of Texas MD Anderson Cancer Center, Houston, TX 77030, USA

[7]Women's Health Integrated Research Center, Women's Service Line, Inova Health System, VA 22003, USA.

*Author's contributed equally

Keywords: high-grade serous ovarian cancer, low-grade serous ovarian cancer, HGSOC, LGSOC, quantitative proteomics, mucin-16, MUC16, cancer antigen 125, CA125, hepatocyte growth factor receptor, focal adhesion kinase

Address correspondence to: Nicholas W. Bateman, email: batemann@whirc.org or Thomas P. Conrads, email: conrads@whirc.org, 3289 Woodburn Rd, Suite 375, Annandale, VA 22003; Tel: 703-207-3357; Fax: 703-560-0919.

Abstract

Low-grade serous ovarian carcinoma (LGSOC) is a rare and largely chemoresistant subtype of epithelial ovarian cancer. Unlike treatment for high-grade serous ovarian cancer (HGSOC), management options for LGSOC patients are limited, in part, due to a lack of deep molecular characterization of this disease. To address this limitation, we performed quantitative mass spectrometry-based proteomic analyses of whole tissue collections of tumors harvested from LGSOC (n=12) and HGSOC (n=24) patients or normal fallopian tube tissues (n=12) from women with benign disease. We quantified 7,043 proteins across all patient samples and unsupervised analyses revealed proteome alterations distinctly stratify fallopian tube tissue, LGSOC, and HGSOC tumors. Proteins elevated in LGSOC compared to HGSOC tumors (LIMMA adjusted $p < 0.05$) were enriched for pathways regulating cilium assembly and included a pathway regulating activation of FAK1 by MET, a therapeutic target in LGSOC. Using data from an independent proteomic analysis of LGSOC (n=14) and HGSOC (n=30) tumors, we identified 330 co-altered proteins between LGSOC and HGSOC tumors exhibiting high quantitative correlation (Spearman Rho = 0.803, $P < 2.2 \times 10^{-16}$). Among these, MUC16 (CA125) was identified as significantly elevated (>1.7 $\log_2$-fold) in LGSOC versus HGSOC. Immunohistochemistry analysis of MUC16 verified the increased abundance in LGSOC tissues and identified that MUC16 staining patterns in LGSOC are uniquely apical compared to HGSOC (Fisher's Exact p = 0.001). Our deep proteomic analyses identifies highly-conserved proteome alterations distinguishing LGSOC from HGSOC tumors, including candidates regulating FAK1 signaling as well as a novel identification that MUC16 is elevated and exhibits an apical staining pattern in LGSOC tumors. These findings deepen our molecular understanding of LGSOC and provide unique insights into the regulation of MUC16 in LGSOC tumors.

61 **Introduction**

62 Despite overall improvements in mortality, ovarian cancer is one of the most lethal gynecologic
63 malignancies, with fewer than half of women surviving five years beyond initial diagnosis[1]. In
64 2024, the American Cancer Society estimates that 19,680 women diagnosed with ovarian cancer
65 and 12,740 (64%) will die from their disease[2]. Epithelial ovarian cancer is the most common
66 histologic subtype of ovarian cancer and includes high-grade serous, low-grade serous, mucinous,
67 clear cell, endometrioid, and carcinosarcoma. High-grade serous ovarian cancer (HGSOC) is the
68 most common histologic subtype and is treated with a combination of cytoreductive surgery and
69 platinum-taxane chemotherapy. Low-grade serous ovarian cancer (LGSOC) is responsible for 2-
70 5% of ovarian cancer and is an overall challenging disease to treat given the high rate of
71 chemoresistance of this disease compared to HGSOC[3].

72 Historically, the hypothesis was that LGSOC ultimately progressed to HGSOC, but this
73 hypothesis has been challenged and current opinion suggests these two disease processes to be
74 independent[4]. From a molecular standpoint, both HGSOC and LGSOC vary by morphology and
75 somatic mutations. HGSOC is associated with *TP53* mutations as opposed to LGSOC, which often
76 harbors mutations in Kirsten rat sarcoma virus (KRAS), the proto-oncogene B-Raf (BRAF),
77 receptor tyrosine-protein kinase erbB-2 (ERBB2), beta-catenin (CTNNB1), as well as
78 phosphatidylinositol 4,5-bisphosphate 3-kinase catalytic subunit alpha isoform (PIK3CA)[4].
79 However, co-existing high-grade and low-grade tumors often exhibit the same mutation and lack
80 a TP53 mutation, suggesting there may be a stepwise, non-TP53 related pathogenic process[4]. More
81 importantly, an understanding of genomic differences between these disease subtypes has also
82 introduced new treatments for LGSOC patients [5].

83

Although the genomic characterization of HGSOC and LGSOC is well established, there is currently limited proteomic data characterizing these tumors. Some hypotheses suggest that fallopian tube epithelium may serve as a site of origin for both LGSOC and HGSOC [3,6], which provides a rationale for its incorporation in the proteomic evaluation of these tumors. As a result, we sought to perform a deep proteomic investigation evaluating tumors from patients diagnosed with LGSOC and HGSOC as well as normal fallopian tube tissues from women with benign disease to better understand the differences in molecular alterations between these tumors and to determine whether there may be any additional pathways and therapeutic targets to help guide further treatment paradigms.

107 **Methods**

108 **Patient cohort and tissue collections**

109 Formalin-fixed, paraffin-embedded (FFPE) LGSOC and HGSOC tumor and normal fallopian tube
110 tissues were obtained from Inova Fairfax Hospital (Falls Church, VA) under a less than minimal-
111 risk WCG IRB-approved protocol #20122048 with waivers for consent and HIPAA authorization
112 and evaluated under protocol #14-1679 with an exempt determination by the WCG IRB in
113 accordance with the use of de-identified data under US Federal regulation 45 CFR 46.102(f).
114 Benign fallopian tube tissues (FT) (n=12), as well as tumor tissues from LGSOC (n=12) and
115 HGSOC (n=24) patients, were sectioned onto 8 µm polyethylene naphthalate membrane slides and
116 hematoxylin-eosin stained. Equivalent areas of whole tissue from FT and tumor epithelium were
117 collected using laser microdissection, avoiding areas of necrosis and hemorrhage, directly into 50
118 µL of Optima™ LC/MS Grade water (Fisher Chemical) in microcentrifuge tubes and stored at -
119 80ºC until sample preparation.

120

121 **Sample preparation for quantitative proteomic analysis**

122 Protein from FFPE tissues was prepared for quantitative mass spectrometry (MS)-based
123 proteomics as previously described[7]. Briefly, tissues were transferred to MicroTubes (Pressure
124 BioSciences, Inc., Easton, MA, USA) including 20 µL of 100 mM TEAB (pH 8.0)/10%
125 acetonitrile and underwent pressure-assisted trypsin digestion employing a barocycler (2320EXT,
126 Pressure BioSciences, Inc.) and a heat-stable form of trypsin (SMART Trypsin, Thermo Fisher
127 Scientific, Inc., Waltham, MA, USA). Peptide digest concentrations were determined using the
128 bicinchoninic acid assay (BCA; Thermo Fisher Scientific, Inc.). Peptides were labeled with
129 isobaric tandem mass tag (TMT) reagents according to the manufacturer's instructions (TMT11™

130 Isobaric Label Reagent Set, Thermo Fisher Scientific). Sample multiplexes were reversed-phase
131 fractionated (basic pH) on a 1260 Infinity II offline liquid chromatography system (Agilent
132 Technologies, Inc., Santa Clara, CA, USA) into 96 fractions using a linear gradient of acetonitrile
133 (0.69% min^{-1}) followed by concatenation into 24 pooled fractions. Pooled fractions were
134 lyophilized in a Speed-Vac and stored at -20 ºC until resuspended in 25 mM NH_4HCO_3 and
135 analyzed by liquid chromatography-tandem mass spectrometry (LC-MS/MS).
136

137 **LC-MS/MS Analysis**

138 Peptide identifications and quantitation for TMT multiplexes were performed as recently
139 described[8]. Liquid chromatography-tandem mass spectrometry (LC-MS/MS) analyses of TMT11
140 multiplexes were performed on a nanoflow high-performance LC system (EASY-nLC 1200,
141 Thermo Fisher Scientific, Inc.) coupled online with an Orbitrap mass spectrometer (Q Exactive
142 HF-X, Thermo Fisher Scientific, Inc.). Samples were loaded on a reversed-phase trap column
143 (Acclaim™ PepMap™ 100 Å, C-18, 20 mm length, nanoViper Trap column, Thermo Fisher
144 Scientific, Inc.) and eluted on a heated (50 °C) reversed-phase analytical column (Acclaim™
145 PepMap™ RSLC C-18, 2 µm, 100 Å, 75 µm × 500 mm, nanoViper, Thermo Fisher Scientific,
146 Inc.) by developing a linear gradient from 2% mobile phase A (2% acetonitrile, 0.1% formic acid)
147 to 32% mobile phase B (95% acetonitrile, 0.1% formic acid) over 120 min at a constant flow rate
148 of 250 nL/min. Full scan mass spectra (MS) were acquired using a mass range of *m/z* 400-1600,
149 followed by selection of the top 12 most intense molecular ions in each MS scan for high-energy
150 collisional dissociation (HCD). Instrument parameters were as follows: Full MS: AGC, 3 × 10e6;
151 resolution, 60 k; S-Lens RF, 40%; max IT, 45 ms; MS2: AGC, 10e5; resolution, 45 k; max IT, 95
152 ms; quadrupole isolation, 1.0 *m/z*; isolation offset, 0.2 *m/z*; NCE, 34; fixed first mass, 100 *m/z*;

153 intensity threshold, 2 × 10e5; charge state, 2–4; dynamic exclusion, 20 s with 10 ppm tolerance,
154 TMT optimization. Global protein-level abundances were generated from peptide spectral matches
155 identified by searching .raw data files against a publicly available, non-redundant human proteome
156 database (http://www.uniprot.org/, SwissProt, Homo sapiens, downloaded 12-01-2017 using
157 Mascot (Matrix Science, v2.6.0), Proteome Discoverer (v2.2.0.388, Thermo Fisher Scientific,
158 Inc.), and in-house tools using identical parameters as previously described[8].
159

160 **Bioinformatic Analysis**

161 Differential analyses of TMT-11 data matrixes were performed using the LIMMA package
162 (version 3.8)[9] in R (version 3.5.2) and Mann-Whitney U rank sum testing in MedCalc (version
163 19.0.3). Pathway analysis was performed using MSigDB and GSEA[10] considering hallmark and
164 canonical pathways using default enrichment settings, i.e. significantly enriched pathways
165 satisfied a false discovery rate < 0.05 or STRING (https://string-db.org/) using default parameters
166 for Homo Sapiens. Visualizations were generated using SRplot[11] , GraphPad Prism (v.10.0.3) or
167 MedCalc. Global proteome data for LGSOC and HGSOC validation cohorts were previously
168 reported[8,12] and HGSOC data prioritized for this analysis was focused on tumors where tissue
169 source site was designated as primary.
170

171 **Immunohistochemical analysis of mucin-16 (MUC16)/ cancer antigen 125 (CA125)**

172 LGSOC and HGSOC tissues were sectioned onto charged glass slides, fixed with 100% methanol,
173 incubated at 5 min at ambient temperature then rinsed with phosphate-buffered saline (PBS).
174 Tissue was permeabilized by incubating with 0.05% triton-PBS for 15 min and 2.5% normal goat
175 serum. The slides were incubated overnight at 4 °C with anti-CA125 mouse monoclonal antibody

176 (Clone M11, Agilent Dako, Santa Clara, CA, USA 1:1000). Dako's Envision diaminobenzidine
177 (DAB) detection system was used to label bound antibody complexes. Normal lung tissue was
178 used as the positive tissue control. Following detection, slides were counterstained with
179 hematoxylin then dehydrated and cover slipped. Stained tissue sections were scanned on an Aperio
180 ScanScope XT slide scanner (Leica Microsystems, Wetzlar, Germany). Digital images underwent
181 expert pathology review (PMF).
182
183
184
185
186
187
188
189
190
191
192
193
194
195
196
197
198

199 **Results**

200 **Quantitative proteomic analyses of whole tissue collections from normal fallopian tube as**
201 **well as low and high-grade serous ovarian cancers.**

202 We performed multiplexed, quantitative proteomic analyses of whole tissue equivalents collected
203 from low-grade (LGSOC, n=12) or high-grade serous ovarian cancers (HGSOC, n=24) tumors and
204 fallopian tube tissues (FT, n=12) from women with benign disease (Figure 1, Supplementary Table
205 1). Global proteomic analyses resulted in the quantitation of 7,043 proteins across all patient
206 samples (Supplementary Table 2). Principal component analysis of top variably abundant proteins
207 quantified across all patient samples explained 40.1% (PC1) and 9.4% (PC2) of the variance
208 between FT, LGSOC and HGSOC tissue collections (Figure 2A). Differential analysis of proteins
209 quantified between HGSOC or LGSOC and FT collections identified both co-altered as well as
210 unique protein alterations between these comparisons (Figure 2B, Supplementary Table 3 and 4).
211 Pathway analysis of co-altered proteins elevated in HGSOC and LGSOC compared to FT
212 identified enrichment of top pathways correlating with regulation of protein translation (i.e., 40S/
213 60S ribosome and eukaryotic translation elongation) as well as protein metabolism (i.e., response
214 of EIF2AK4 to amino acid deficiency and selenoamino acid metabolism) in tumor samples (Figure
215 2C, Supplementary Table 5). Pathways enriched among proteins elevated in FT tissues largely
216 correlated with regulation of cilium development as well as organelle biogenesis (Figure 2C,
217 Supplementary Table 5). Pathway analysis of proteins uniquely elevated in HGSOC identified
218 pathways largely associated with cell cycle regulation while pathways enriched for proteins
219 uniquely elevated in LGSOC tumors correlated with pathways regulating epithelial to
220 mesenchymal transition and hematopoietic related signaling (Figure 2D, Supplementary Table 6).
221

222 **Characterization and validation of proteome alterations between low and high-grade serous**
223 **ovarian cancers**

224 Differential analysis of proteins quantified in LGSOC and HGSOC tumors identified 785 proteins
225 as significantly altered between these tumor types (Figure 3A). Top protein alterations included
226 proliferation marker protein Ki-67 (MKI67) elevated in HGSOC and multiple collagen isoforms
227 in LGSOC tumors (Figure 3A, Supplementary Table 7). Comparison of these protein alterations
228 with global proteome data recently described for an independent cohort of tumor tissues collected
229 from women diagnosed with LGSOC[12] (n=14) or HGSOC[8] (n=30) tumors identified 330 protein
230 features as co-altered between these disease subtypes that further exhibit high quantitative
231 correlation (Figure 3B, Supplementary Table 8). Pathway analysis of 313 proteins within this
232 subset exhibiting concordant abundance trends showed proteins elevated in LGSOC tumors are
233 enriched for pathways regulating cilium development as well as focal adhesions and, specifically,
234 regulation of focal adhesion kinase 1 (FAK1/ PTK2) by hepatocyte growth factor receptor (MET)
235 (Figure 3C). Proteins elevated in HGSOC tumors showed enrichment of pathways largely
236 regulating cell cycle and cellular mitosis (Figure 3C, Supplementary Table 9). Investigation of
237 putative drug targets among proteins co-altered between LGSOC and HGSOC tumors in both
238 discovery and validation cohorts identified 34 candidates (Supplementary Table 8). Putative drug
239 targets elevated in HGSOC tumors included several proteins known to regulate DNA replication[13],
240 i.e. DNA topoisomerase IIα (TOP2A) and polymerase delta 1 (POLD1) while those elevated in
241 LGSOC tumors included diverse candidates like hepatocyte growth factor receptor (MET),
242 targeted by diverse receptor tyrosine kinase inhibitors[14] as well as mucin-16 (MUC-16), also
243 known as cancer antigen 125 (CA125, Figure 3D). Circulating MUC16/CA125 levels are assessed
244 as part of routine diagnosis and disease monitoring in the clinical management of ovarian cancer[3,6].

245 To uncover whether other putatively conserved protein candidates elevated in LGSOC tumors are
246 predicted to interact with MUC16, we investigated these protein features using the STRING
247 interaction network (string-db.org). We identified nesprin-1 (SYNE1), mucin-5B (MUC5B) and
248 galecin-3 (LGALS3) as putative interactome partners of MUC16 and all significantly elevated in
249 LGSOC tumors (Supplementary Table 8). Considering the importance of MUC16 in ovarian
250 cancer disease biology, we were motivated to investigate this protein alteration in LGSOC and
251 HGSOC tissues further.
252

253 **Mucin-16 (MUC16)/ cancer antigen 125 (CA125) is elevated and exhibits a predominantly**
254 **apical staining pattern in low versus high-grade serous ovarian cancers**

255 To further investigate elevation of MUC16 protein as a putatively conserved protein alteration in
256 LGSOC versus HGSOC tumors, we performed immunohistochemistry (IHC) analysis of tissues
257 for a subset of LGSOC (n=11) and HGSOC (n=24) tumors characterized within our discovery
258 cohort. A comparison of tumor cells stained positive for MUC16 between LGSOC and HGSOC
259 tumors showed HGSOC tumors overall have fewer MUC16-positive cells than LGSOC cells
260 (Figure 4A, Supplementary Table 10). Further analysis of MUC16 staining identified discrete
261 localization patterns correlating with disease subtypes, where HGSOCs exhibited a more
262 membranous or combined apical and membranous staining pattern while LGSOCs exhibited a
263 predominantly apical MUC16 staining pattern (Figure 4B). We further include MUC16 IHC
264 images for two representative HGSOC cases demonstrating apical and membranous staining as
265 well as for two LGSOC cases, which exhibit a predominant and intense, apical membrane staining
266 pattern (Figure 4C).
267

268 **Discussion**

269 Our deep proteomic analysis of benign fallopian tube tissues as well as low (LGSOC) and high
270 (HGSOC) grade serous ovarian cancers shows these samples can be stratified by variably abundant
271 protein alterations suggesting distinct proteome abundance profiles are characteristic of these
272 tissue types. Differential analysis of tumor (LGSOC and HGSOC) and benign fallopian tube tissue
273 identified that proteins elevated in fallopian tubes were largely enriched for pathways regulating
274 cilium development. Recent evidence from single cell studies has identified several subpopulations
275 of epithelial cell types exist within benign fallopian tube, including ciliated cell types[15,16]. This cell
276 population is considered to reflect a more differentiated subpopulation of fallopian tube epithelial
277 cells emerging from non-ciliated, secretory epithelial cell types[15,16]. The loss of proteins regulating
278 cilium development that we observe in LGSOC and HGSOC tissues is consistent with evidence
279 suggesting secretory epithelial cell types often exhibit greater neoplastic potential than other cell
280 types in fallopian tube epithelium[15]. We also find that proteins elevated in both LGSOC and
281 HGSOC tumors exhibit enrichment of pathways regulating protein translation, specifically
282 ribosome and translational elongation, as well as amino acid metabolism in comparison with
283 benign fallopian tube. Increased ribosome biogenesis and protein translation has been described
284 as being characteristic of ovarian cancer cells and has further been suggested as a possible
285 therapeutic vulnerability in both LGSOC and HGSOC[17,18]. Proteins uniquely elevated in HGSOC
286 tumors compared to benign fallopian tube were largely enriched for pathway regulating cell cycle
287 and mitosis, consistent with the high-grade phenotype of this disease[19]. Proteins uniquely elevated
288 in LGSOC were enriched for pathways regulating epithelial to mesenchymal transition including
289 extracellular matrix organization, beta1 integrin cell surface interactions and hematopoietic-related
290 signaling, i.e. complement and coagulation. Beta1 integrin signaling has been implicated in

291 regulating migration of ovarian cancer cells in the context of interactions with extracellular matrix
292 proteins[20]. Our comparison with fallopian tube tissues has identified proteome alterations largely
293 consistent with the malignant phenotypes of LGSOC and HGSOC tumors in comparison to benign
294 fallopian tube.

295 Comparison of LGSOC and HGSOC revealed marked protein alterations between these
296 disease subtypes, including elevation of proteins correlating with proliferation and DNA
297 replication in HGSOC. We also observe elevation of diverse extracellular matrix proteins in
298 LGSOC tumors, including multiple collagen isoforms which is consistent with the enrichment of
299 epithelial to mesenchymal signaling pathways[21] we also observed in these tumors. Our team
300 recently described global proteome analysis of tumors collected from women diagnosed with
301 LGSOC[12] or with HGSOC[8] and we were motivated to compare proteome alterations we have
302 observed between LGSOC and HGSOC tumors from this study with these independent cohorts to
303 identify and validate proteome alterations that are highly conserved between these disease
304 subtypes. This comparison resulted in the identification of a subset of protein alterations exhibiting
305 high quantitative correlation between LGSOC and HGSOC tumors (Spearman Rho > 0.8). These
306 features demonstrated that proteins elevated in HGSOC tumors largely correlate with enrichment
307 of pathways regulating cell cycle and cell mitosis signaling, while those elevated in LGSOC
308 tumors correlated with intercellular and extracellular matrix interactions, i.e. focal adhesion and
309 laminin interactions, but also included enrichment of pathways regulating cilium development as
310 well as regulation of focal adhesion kinase 1 (FAK/ PTK2) by hepatocyte growth factor receptor
311 (MET). Investigation of protein alterations mapping to this latter pathway shows that MET, but
312 not FAK, is significantly elevated in LGSOC versus HGSOC tumors (Supplementary Table 8).
313 MET is a receptor tyrosine kinase that can signal through phosphoinositide 3-kinase (PI3K) or

314 mitogen activated protein kinase (MAPK) pathways resulting in increased survival and invasive
315 potential of tumor cells[22,23]. MET has been shown to be elevated in ovarian cancer cells and
316 activated by increased hepatocyte growth factor production from cancer associated fibroblasts that
317 is further correlated with a chemoresistant phenotype[24]. FAK has been found to promote
318 oncogenesis in diverse cancers including ovarian by increasing the invasive potential of tumor
319 cells through extracellular matrix remodeling as well as by modulating PI3K and MAPK signaling
320 pathways to promote tumor cell aggressivity[25,26]. Notably, MAPK signaling has been shown to be
321 hyperactivated in LGSOC tumors[3,26] and targeting MAPK signaling using clinical inhibitors of
322 MAPK signaling, i.e. MEK inhibitors has led to multiple clinical trials focused on exploiting this
323 therapeutic vulnerability in LGSOC[3,26]. Recent evidence has shown that activation of FAK can
324 promote resistance to MEK inhibitors[27] and this has led to clinical trials combining MEK inhibitors
325 with the FAK inhibitor Defactinib to treat LGSOC, including a phase 2 trial focused on leveraging
326 this combination therapy for the treatment of recurrent LGSOC (ENGOT-ov60/GOG-3052/RAMP
327 201, i.e. NCT04625270)[26]. Our findings provide further supportive evidence that elevation of MET
328 protein abundance as well as enrichment of pathways correlating with FAK signaling is highly
329 conserved in LGSOC tumors.

330 Additional investigation of putatively conserved protein alterations between LGSOC and
331 HGSOC tumors identified mucin-16 (MUC16)/ cancer antigen 125 (CA125) as significantly
332 elevated in LGSOC versus HGSOC tumor tissues. MUC16 is a transmembrane glycoprotein that
333 is highly abundant in the female reproductive tract and can be actively shed from ovarian cancer
334 cells into blood plasma[6]. Circulating MUC16/ CA125 protein levels thus represents a biomarker
335 that can be measured to assess evidence of disease and is a facet of routine diagnosis and disease
336 monitoring in the clinical management of ovarian cancer[3,6]. Shedding of MUC16 has been shown

337 to occur as a product of proteolytic cleavage of the carboxy-terminal ectodomain in the acidifying
338 Golgi/ post-Golgi[28], possibly by membrane-type 1 matrix metalloproteinase[29] followed by release
339 of the N-terminal CA125 region[29] into interstitial fluid and ultimately into circulating blood[6]. As
340 we quantify membrane-type 1 matrix metalloproteinase (MT1-MMP/ MMP-14/ P50281) protein
341 in our discovery cohort, we compared levels between LGSOC &HGSOC tumors, but we do not
342 observe this protein as significantly altered between these disease subtypes (MWU $p = 0.48$).
343 Recent evidence investigating mechanisms regulating cell surface retention of MUC16 have
344 implicated N-glycosylation mediated by N-acetylglucosaminyltransferase I (MGAT1) that
345 promotes increased retention of MUC16 at the cell surface[30]. This study further identified N-
346 glycosylation of MUC16 promotes interaction with the protein galectin-3 (LGALS3) at the cell
347 surface[30]. Notably, we identify LGALS3 as significantly elevated in LGSOC versus HGSOC
348 tumor tissues and, although we quantify MGAT1, we do not see this protein as significantly altered
349 between LGSOC versus HGSOC tissues (Supplementary Table 7). Considering this evidence in
350 the context of our findings suggests LGSOC tumor cells perhaps exhibit increased retention of
351 MUC16 at the cell surface. Circulating CA125 levels have been observed in both LGSOC and
352 HGSOC patients, although it has been noted that these levels are more commonly lower in LGSOC
353 patients[3,31]. We also find that circulating CA125 levels were lower in our LGSOC versus HGSOC
354 patients (Table 1), providing further evidence in support of this hypothesis. A possible mechanism
355 underlying altered dynamics of MUC16 retention may be due to differential N-glycosylation of
356 MUC16 in LGSOC tumor cells, possibly due to altered enzymatic activity of MGAT1.
357 Alternatively, differences in MUC16 expression and shedding could relate to greater cleavage of
358 the extracellular domain in HGSOC, accounting for the greater shedding of CA125 and decreased

359 membrane expression. Future studies will focus on investigation of these hypothesis including
360 comparison of cleaved versus non-cleaved MUC16 levels in LGSOC and HGSOC tumors.

361 We also observe that LGSOC tumor cells exhibit a predominantly apical staining pattern
362 for MUC16 in comparison to HGSOC tumor cells. Similar findings were observed in murine
363 ovarian carcinomas where more intense apical expression of MUC16 was observed in grade 1
364 tumors[32]. Recent evidence has shown that MUC16 is maintained within apical membranes of
365 epithelial cells, such as in ocular epithelium[33], and to be dependent on glycosylation[30], which when
366 considered relative to our findings may explain why we observe increased apical staining patterns
367 for MUC16 in LGSOC tissues. Beyond its role as a biomarker, MUC16 has been shown to promote
368 cellular proliferation and invasion of ovarian cancer cells[34] and has previously been shown to
369 discourage immune surveillance and to be a potential target for immunotherapy[35]. Future efforts
370 will be focused on not only investigating mechanisms of membrane retention of MUC16 in
371 LGSOC, but further on improving our understanding of how this characteristic impacts LGSOC
372 tumor cell biology.

373 A limitation for the current study includes small sample sizes for normal fallopian tube as
374 well as LGSOC and HGSOC tissues in our discovery cohort. We aimed to address this limitation
375 by prioritizing protein alterations between LGSOC and HGSOC tumors that were further validated
376 within global proteomic data generated for independent cohorts of LGSOC and HGSOC patients.
377 One may also claim another limitation is that samples were obtained by formalin-fixed, paraffin-
378 embedded tissue instead of fresh frozen tissue. Nevertheless, comparison of fresh tissue samples
379 and fixed frozen paraffin embedded samples has not demonstrated differences in peptide
380 identification and quantification[36]. Strengths of this study include the foundation provided for

381 future proteomic research, and the contributions of our findings towards improving our
382 understanding of molecular alterations underlaying ovarian cancer pathogenesis.
383
384 **Conclusion**
385 Our study contributes to our understanding of global proteome dynamics between normal fallopian
386 tube tissues and LGSOC and HGSOC tumors and provide insights into the relative abundance and
387 localization of the ovarian cancer biomarker MUC16/ CA125 in LGSOC and HGSOC tumors that
388 may have bearing on clinical interpretation of circulating levels of CA125 in these disease
389 subtypes. Future study is needed to determine the significance of protein alterations in the course
390 of this disease, and which—if any—proteins may serve as additional therapeutic targets for disease
391 treatment.
392

393 **Table 1: Patient and tumor clinicopathological characteristics**

Characteristic	High Grade Serous Ovarian Cancer (N = 24)	Low Grade Serous Ovarian Cancer (N = 12)	Benign Fallopian Tube (N = 12)
Mean age (range) –yr	58.1 (30-90)	52.0 (30-73)	45.2 (41-49)
Menopausal status – no. (%)			
Premenopausal	5 (20.8)	6 (50.0)	12 (100.0)
Postmenopausal	19 (79.2)	6 (50.0)	0 (0.0)
Mean BMI (range)	25.6 (22.5 – 30)	25.4 (20.7 – 30.8)	30.1 (19 – 44.1)
Race – no. (%)			
White	13 (54.2)	11 (91.7)	4 (33.3)
Black	7 (29.2)	0 (0.0)	4 (33.3)
Asian	4 (16.7)	1 (8.3)	2 (16.7)
Hispanic	0 (0.0)	0 (0.0)	2 (16.7)
FIGO stage – no. (%)			
I or II	2 (8.3)	3 (25.0)	-
IIIA	3 (12.5)	4 (33.3)	-
IIIB	6 (25.0)	1 (8.4)	-
IIIC	7 (29.2)	4 (33.3)	-
IV	6 (25.0)	0 (0.0)	-
Debulking			
RD0	12 (50.0)	7 (58.3)	-
RD1	9 (37.5)	4 (33.3)	-
Suboptimal	2 (8.3)	1 (8.4)	-
Unknown	1 (4.2)	0 (0.0)	-
Platinum Sensitivity – no (%)			
Sensitive	14 (58.3)	8 (66.6)	-
Resistant	4 (16.7)	1 (8.4)	-
Unknown	6 (25.0)	3 (25.0)	-
Mean CA125 (range)	4917.1 (329 – 50,000)	672.7 (70 – 1576)	-

394

395

396

397 **Data Availability**

398 Proteomic data generated in this study is accessible at the ProteomeXChange under accession
399 PXD050642.

400 **Author Contributions**

401 C.M.T., N.W.B., T.P.C. lead the study. C.M.T, P.F., J.O., G.L.M. performed identification of
402 clinical specimens, C.M.T., G.L.M., K.M.D performed clinical data analysis. K.A.C., J.O., and
403 C.M.T. performed sample collections and molecular extraction. N.W.B., J.O., T.A., B.L.H,
404 generated and analyzed proteomics data. P.M.F. performed pathology review. C.M.T., N.W.B.,
405 wrote the manuscript, P.M.F., T.A., B.L.H, K.R., K.K.W, D.G., S.L., A.K.S., R.C.B, K.M.D.,
406 N.T.P, G.L.M, T.P.C reviewed the manuscript. All authors reviewed and approved the final
407 manuscript.

408 **Declaration of Interests**

409 Nothing to disclose.

410 **Acknowledgements**

411 Funding for this project was provided from the Uniformed Services University of the Health
412 Sciences from the Defense Health Program to the Henry M Jackson Foundation (HJF) for the
413 Advancement of Military Medicine Inc. Gynecologic Cancer Center of Excellence Program,
414 including awards HU0001-20-2-0033, HU0001-21-2-0027, HU0001-22-2-0016, and HU0001-23-
415 2-0038 (PI: Neil T Phippen, Co-PI: G. Larry Maxwell).

416

417

418 **Disclaimer**

419 The views expressed herein are those of the authors and do not reflect the official policy of the
420 Uniformed Services University of the Health Sciences, the Henry M. Jackson Foundation for the
421 Advancement of Military Medicine, Inc., Inova Health System, the Department of Army/Navy/Air
422 Force, Department of Defense, or U.S. Government. Mention of trade names, commercial
423 products, or organizations does not imply endorsement by the U.S. Government.

424

425

426 **References**

427 1 Torre, L. A. *et al.* Ovarian cancer statistics, 2018. *CA Cancer J Clin* **68**, 284-296,
428 doi:10.3322/caac.21456 (2018).
429 2 Siegel, R. L., Giaquinto, A. N. & Jemal, A. Cancer statistics, 2024. *CA Cancer J Clin* **74**,
430 12-49, doi:10.3322/caac.21820 (2024).
431 3 Slomovitz, B. *et al.* Low-grade serous ovarian cancer: State of the science. *Gynecol*
432 *Oncol* **156**, 715-725, doi:10.1016/j.ygyno.2019.12.033 (2020).
433 4 Zarei, S. *et al.* Clinicopathologic, Immunohistochemical, and Molecular Characteristics
434 of Ovarian Serous Carcinoma With Mixed Morphologic Features of High-grade and
435 Low-grade Serous Carcinoma. *Am J Surg Pathol* **44**, 316-328,
436 doi:10.1097/PAS.0000000000001419 (2020).
437 5 Gershenson, D. M. *et al.* Trametinib versus standard of care in patients with recurrent
438 low-grade serous ovarian cancer (GOG 281/LOGS): an international, randomised, open-
439 label, multicentre, phase 2/3 trial. *Lancet* **399**, 541-553, doi:10.1016/S0140-
440 6736(21)02175-9 (2022).
441 6 Giamougiannis, P., Martin-Hirsch, P. L. & Martin, F. L. The evolving role of MUC16
442 (CA125) in the transformation of ovarian cells and the progression of neoplasia.
443 *Carcinogenesis* **42**, 327-343, doi:10.1093/carcin/bgab010 (2021).
444 7 Burdett, N. L. *et al.* Multiomic analysis of homologous recombination-deficient end-stage
445 high-grade serous ovarian cancer. *Nat Genet* **55**, 437-450, doi:10.1038/s41588-023-
446 01320-2 (2023).
447 8 Lee, S. *et al.* Molecular Analysis of Clinically Defined Subsets of High-Grade Serous
448 Ovarian Cancer. *Cell Rep* **31**, 107502, doi:10.1016/j.celrep.2020.03.066 (2020).
449 9 Ritchie, M. E. *et al.* limma powers differential expression analyses for RNA-sequencing
450 and microarray studies. *Nucleic Acids Res* **43**, e47, doi:10.1093/nar/gkv007 (2015).
451 10 Subramanian, A. *et al.* Gene set enrichment analysis: a knowledge-based approach for
452 interpreting genome-wide expression profiles. *Proc Natl Acad Sci U S A* **102**, 15545-
453 15550, doi:10.1073/pnas.0506580102 (2005).
454 11 Tang, D. *et al.* SRplot: A free online platform for data visualization and graphing. *PLoS*
455 *One* **18**, e0294236, doi:10.1371/journal.pone.0294236 (2023).
456 12 Wong, K. K. *et al.* Integrated multi-omic analysis of low-grade ovarian serous carcinoma
457 collected from short and long-term survivors. *J Transl Med* **20**, 606, doi:10.1186/s12967-
458 022-03820-x (2022).
459 13 Ganai, R. A. & Johansson, E. DNA Replication-A Matter of Fidelity. *Mol Cell* **62**, 745-
460 755, doi:10.1016/j.molcel.2016.05.003 (2016).
461 14 Huang, X. *et al.* Targeting the HGF/MET Axis in Cancer Therapy: Challenges in
462 Resistance and Opportunities for Improvement. *Front Cell Dev Biol* **8**, 152,
463 doi:10.3389/fcell.2020.00152 (2020).
464 15 Dinh, H. Q. *et al.* Single-cell transcriptomics identifies gene expression networks driving
465 differentiation and tumorigenesis in the human fallopian tube. *Cell Rep* **35**, 108978,
466 doi:10.1016/j.celrep.2021.108978 (2021).
467 16 Ghosh, A., Syed, S. M. & Tanwar, P. S. In vivo genetic cell lineage tracing reveals that
468 oviductal secretory cells self-renew and give rise to ciliated cells. *Development* **144**,
469 3031-3041, doi:10.1242/dev.149989 (2017).
470 17 Yan, S. *et al.* The Potential of Targeting Ribosome Biogenesis in High-Grade Serous
471 Ovarian Cancer. *Int J Mol Sci* **18**, doi:10.3390/ijms18010210 (2017).

18 Kang, J. *et al.* Ribosomal proteins and human diseases: molecular mechanisms and targeted therapy. *Signal Transduct Target Ther* **6**, 323, doi:10.1038/s41392-021-00728-8 (2021).
19 Lopez-Reig, R. & Lopez-Guerrero, J. A. The hallmarks of ovarian cancer: proliferation and cell growth. *EJC Suppl* **15**, 27-37, doi:10.1016/j.ejcsup.2019.12.001 (2020).
20 Casey, R. C. & Skubitz, A. P. CD44 and beta1 integrins mediate ovarian carcinoma cell migration toward extracellular matrix proteins. *Clin Exp Metastasis* **18**, 67-75, doi:10.1023/a:1026519016213 (2000).
21 Yi, B. R., Kim, T. H., Kim, Y. S. & Choi, K. C. Alteration of epithelial-mesenchymal transition markers in human normal ovaries and neoplastic ovarian cancers. *Int J Oncol* **46**, 272-280, doi:10.3892/ijo.2014.2695 (2015).
22 Kim, H. J. Therapeutic Strategies for Ovarian Cancer in Point of HGF/c-MET Targeting. *Medicina (Kaunas)* **58**, doi:10.3390/medicina58050649 (2022).
23 Organ, S. L. & Tsao, M. S. An overview of the c-MET signaling pathway. *Ther Adv Med Oncol* **3**, S7-S19, doi:10.1177/1758834011422556 (2011).
24 Di Renzo, M. F. *et al.* Overexpression of the Met/HGF receptor in ovarian cancer. *Int J Cancer* **58**, 658-662, doi:10.1002/ijc.2910580507 (1994).
25 Wu, Y. *et al.* Focal adhesion kinase inhibitors, a heavy punch to cancer. *Discov Oncol* **12**, 52, doi:10.1007/s12672-021-00449-y (2021).
26 Zwimpfer, T. A. *et al.* Low grade serous ovarian cancer - A rare disease with increasing therapeutic options. *Cancer Treat Rev* **112**, 102497, doi:10.1016/j.ctrv.2022.102497 (2023).
27 Taylor, K. N. & Schlaepfer, D. D. Adaptive Resistance to Chemotherapy, A Multi-FAK-torial Linkage. *Mol Cancer Ther* **17**, 719-723, doi:10.1158/1535-7163.MCT-17-1177 (2018).
28 Das, S. *et al.* Membrane proximal ectodomain cleavage of MUC16 occurs in the acidifying Golgi/post-Golgi compartments. *Sci Rep* **5**, 9759, doi:10.1038/srep09759 (2015).
29 Bruney, L., Conley, K. C., Moss, N. M., Liu, Y. & Stack, M. S. Membrane-type I matrix metalloproteinase-dependent ectodomain shedding of mucin16/ CA-125 on ovarian cancer cells modulates adhesion and invasion of peritoneal mesothelium. *Biol Chem* **395**, 1221-1231, doi:10.1515/hsz-2014-0155 (2014).
30 Taniguchi, T. *et al.* N-Glycosylation affects the stability and barrier function of the MUC16 mucin. *J Biol Chem* **292**, 11079-11090, doi:10.1074/jbc.M116.770123 (2017).
31 But, I. & Gorisek, B. Preoperative value of CA 125 as a reflection of tumor grade in epithelial ovarian cancer. *Gynecol Oncol* **63**, 166-172, doi:10.1006/gyno.1996.0301 (1996).
32 Wang, Y. *et al.* MUC16 expression during embryogenesis, in adult tissues, and ovarian cancer in the mouse. *Differentiation* **76**, 1081-1092, doi:10.1111/j.1432-0436.2008.00295.x (2008).
33 Mantelli, F. & Argueso, P. Functions of ocular surface mucins in health and disease. *Curr Opin Allergy Clin Immunol* **8**, 477-483, doi:10.1097/ACI.0b013e32830e6b04 (2008).
34 Felder, M. *et al.* MUC16 (CA125): tumor biomarker to cancer therapy, a work in progress. *Mol Cancer* **13**, 129, doi:10.1186/1476-4598-13-129 (2014).

516 35 Zhai, Y. *et al.* MUC16 affects the biological functions of ovarian cancer cells and induces
517 an antitumor immune response by activating dendritic cells. *Ann Transl Med* **8**, 1494,
518 doi:10.21037/atm-20-6388 (2020).
519 36 Bateman, N. W. & Conrads, T. P. Recent advances and opportunities in proteomic
520 analyses of tumour heterogeneity. *J Pathol* **244**, 628-637, doi:10.1002/path.5036 (2018).

521

522

523 **Figure Legends**

524 **Figure 1: Workflow supporting quantitative proteomic analyses and validation of proteome**
525 **alterations in low (LGSOC) and high-grade (HGSOC) serous ovarian cancers.** Whole tissue
526 collections from benign fallopian tube, LGSOC and HGSOC tissues was performed using laser
527 microdissection. Tissue collections underwent multiplexed, quantitative proteomic analysis using
528 isobaric tagging, i.e. tandem mass tags (TMT-11), followed by liquid chromatography, tandem
529 mass spectrometry (LC-MS/MS) analysis on an Orbitrap mass spectrometer. Proteome alterations
530 identified in discovery cohorts of LGSOC and HGSOC tissues were validated using global
531 proteome data for independent cohorts of LGSOC[12] (n=14) and HGSOC[8] (n=30) tumors and
532 included the finding that mucin-16 (MUC16) is elevated in LGSOC tumors which was further
533 verified by immunohistochemistry analysis of LGSOC and HGSOC tissues.

534

535 **Figure 2: Differential proteomic analysis of whole tissue collections from normal fallopian**
536 **tube with low (LGSOC) and high-grade (HGSOC) serous ovarian cancers.** A: Principal
537 component analysis (PCA) of the top 500 most variably abundant proteins quantified across
538 samples; proteins prioritized based on median absolute deviation. B: Comparison of proteins
539 significantly altered between HGSOC or LGSOC and benign fallopian tube collections; proteins
540 reflect LIMMA adjusted p-value < 0.05, fold-change $\pm$ 2.0. C: Pathway analysis of proteins co-
541 altered between HGSOC and LGSOC vs benign fallopian tube collections; top hallmark and
542 canonical pathways (gsea-msigdb.org) enriched among proteins elevated (84) or decreased (457)
543 in HGSOC and LGSOC versus benign fallopian tube collections. D: Pathway analysis of proteins
544 uniquely elevated in HGSOC or LGSOC vs normal fallopian tube collections; top hallmark and

545 canonical pathways (gsea-msigdb.org) enriched among proteins elevated in HGSOC (300) or
546 LGSOC (158) tumors versus benign fallopian tube collections.

547

548 **Figure 3: Differential proteomic analysis of low (LGSOC) and high-grade (HGSOC) serous**
549 **ovarian cancers and validation of proteome alterations in independent LGSOC and HGSOC**
550 **cohorts.** A: Volcano plot reflects proteins significantly altered between LGSOC and HGSOC
551 tumors; proteins reflect LIMMA adjusted p-value < 0.05, fold-change ± 1.5. B: Proteins co-altered
552 between LGSOC and HGSOC tumors in discovery and validation cohorts; 330 proteins exhibiting
553 LIMMA adjusted p-value < 0.05, fold-change ± 1.5. C: Pathway analysis of proteins co-altered
554 between LGSOC and HGSOC tumors in discovery and validation cohorts; top hallmark and
555 canonical pathways (gsea-msigdb.org) enriched among proteins elevated (144) or decreased (169)
556 between LGSOC and HGSOC tumors. D: Mucin-16 (MUC16) protein abundance in LGSOC and
557 HGSOC tumors from discovery or validation cohorts; * = LIMMA adjusted p-value < 0.05, ****
558 = LIMMA adjusted p-value < 1E-4.

559

560 **Figure 4: Immunohistochemical analysis of Mucin-16 (MUC16) in low (LGSOC) and high-**
561 **grade (HGSOC) serous ovarian cancers.** A: Comparison of cells stained positive for MUC16
562 following immunohistochemical analysis of LGSOC (n=11) and HGSOC (n=24) tissues; p-value
563 reflects Mann Whitney Rank Sum testing. B: Comparison of MUC16 staining patterns in LGSOC
564 (n=11) and HGSOC (n=24) tissues; tumor cell populations were identified to exhibit
565 predominantly apical, membranous or both apical and membranous patterns of MUC16 staining.

566 C: MUC16 immunohistochemistry stains in tissue sections from two representative LGSOC and
567 HGSOC patient tumors.

568

569 **Supplementary Tables**

570 1) Supplementary Table 1 (S1): Discovery cohort details
571 2) Supplementary Table 2 (S2): Global proteome matrix
572 3) Supplementary Table 3 (S3): Differential analysis of LGSOC vs Fallopian Tube
573 4) Supplementary Table 4 (S4): Differential analysis of HGSOC vs Fallopian Tube
574 5) Supplementary Table 5 (S5): Pathway analysis of proteins altered between HGSOC and
575 LGSOC vs Fallopian Tube.
576 6) Supplementary Table 6 (S6): Pathway analysis of proteins uniquely elevated in HGSOC or
577 LGSOC tumors vs Fallopian Tube.
578 7) Supplementary Table 7 (S7): Differential analysis of LGSOC vs HGSOC
579 8) Supplementary Table 8 (S8): Proteins co-altered in LGSOC vs HGSOC between discovery
580 and validation cohorts.
581 9) Supplementary Table 9 (S9): Pathway analysis of proteins altered between HGSOC and
582 LGSOC tumors.
583 10) Supplementary Table 10 (S10): MUC16 immunohistochemistry analysis

Figure1

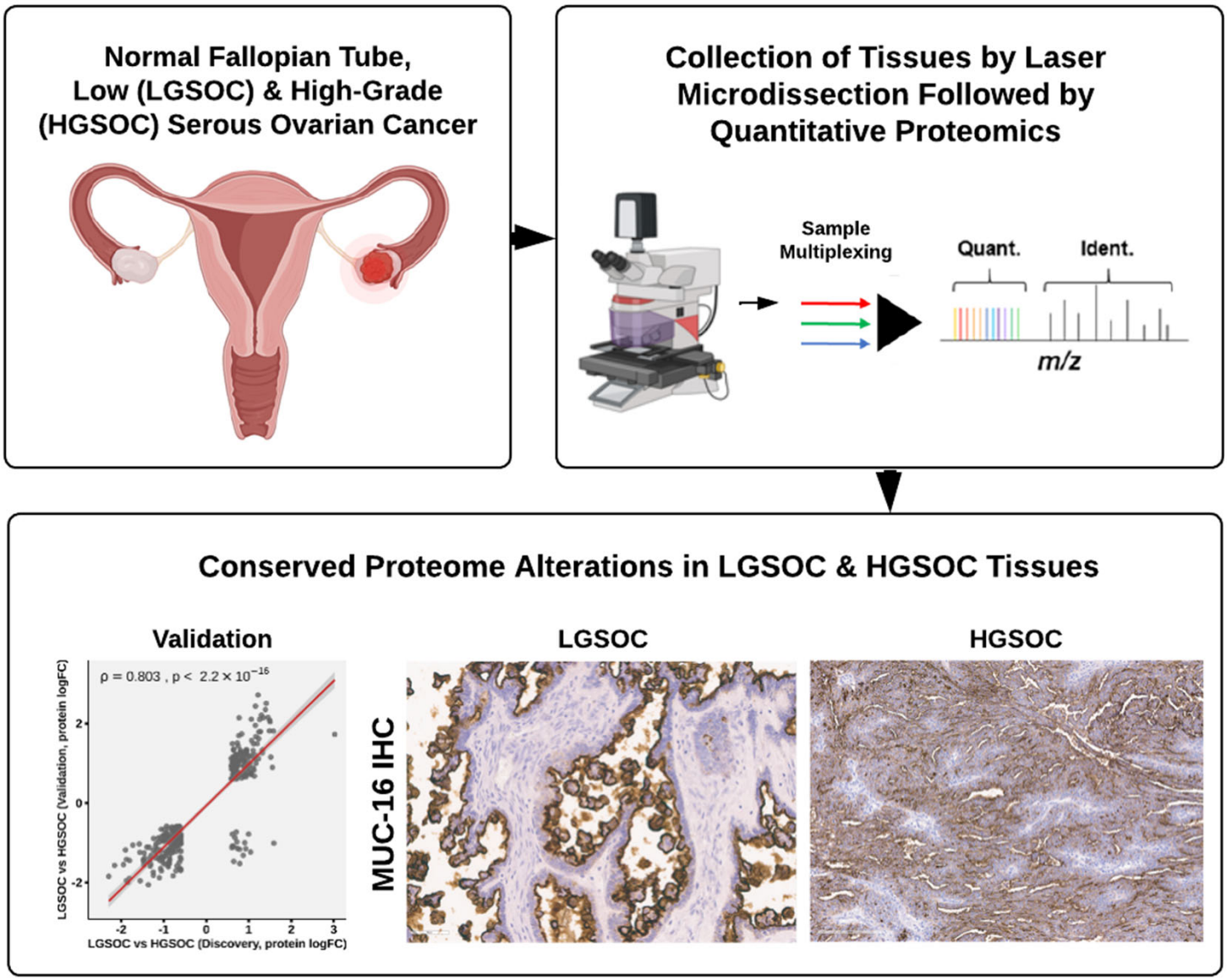
Normal Fallopian Tube, Low (LGSOC) & High-Grade (HGSOC) Serous Ovarian Cancer
Collection of Tissues by Laser Microdissection Followed by Quantitative Proteomics
Sample Multiplexing
Quant.
Ident.
m/z
Conserved Proteome Alterations in LGSOC & HGSOC Tissues
Validation
ρ = 0.803 , p < 2.2 × 10^-16
LGSOC vs HGSOC (Validation, protein logFC)
LGSOC vs HGSOC (Discovery, protein logFC)
LGSOC
HGSOC
MUC-16 IHC

Figure 2

A

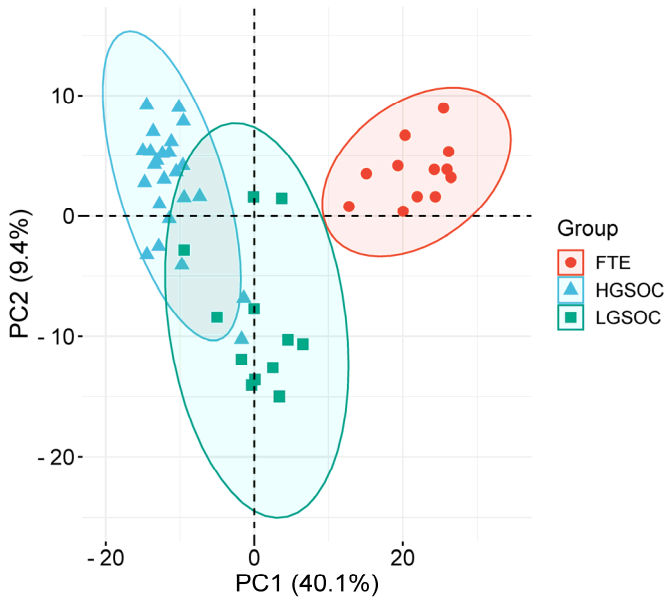

B

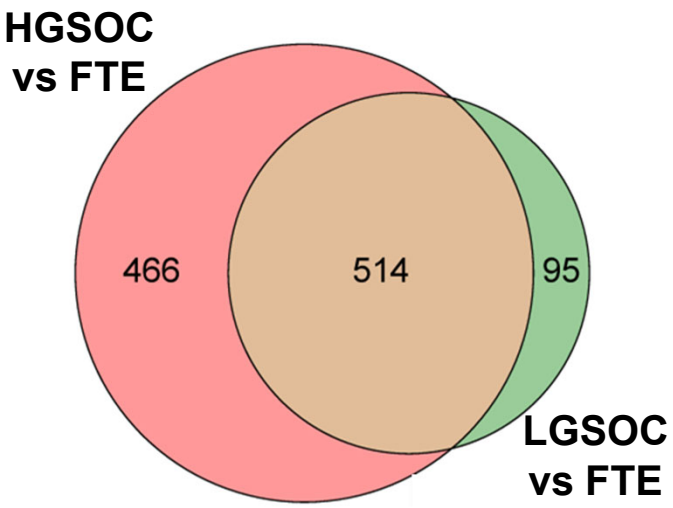

C

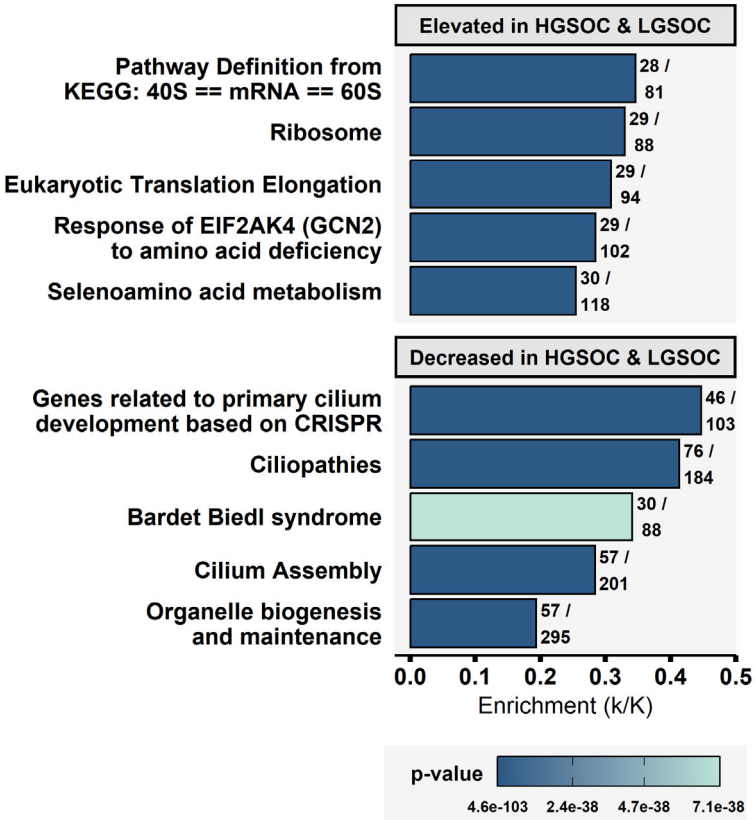

D

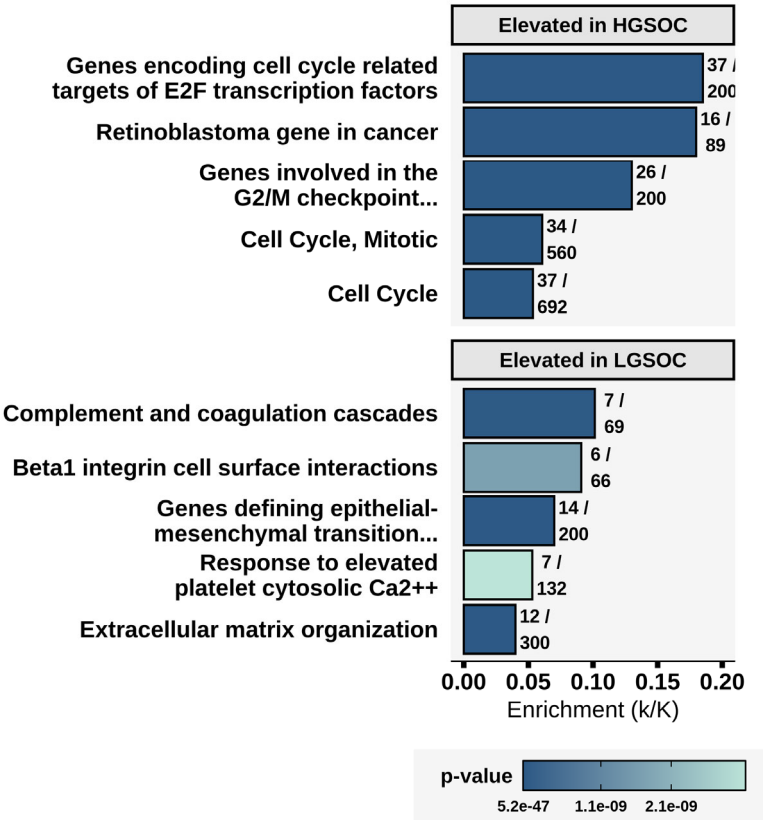

Figure 3

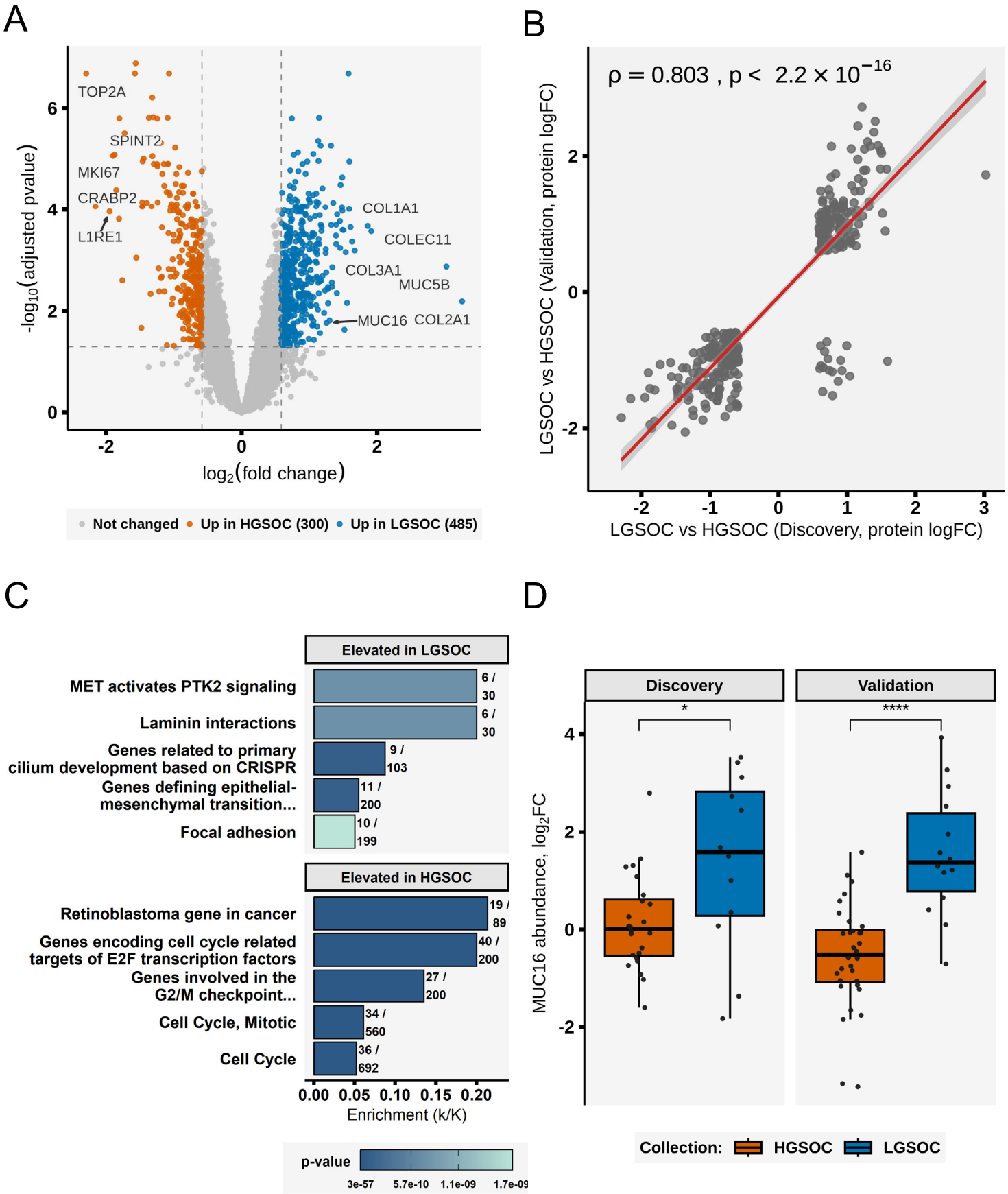
A
TOP2A
SPINT2
MKI67
CRABP2
L1RE1
COL1A1
COLEC11
COL3A1
MUC5B
MUC16
COL2A1
-log10(adjusted pvalue)
log2(fold change)
Not changed
Up in HGSOC (300)
Up in LGSOC (485)
B
ρ = 0.803 , p < 2.2 × 10−16
LGSOC vs HGSOC (Validation, protein logFC)
LGSOC vs HGSOC (Discovery, protein logFC)
C
Elevated in LGSOC
MET activates PTK2 signaling
Laminin interactions
Genes related to primary cilium development based on CRISPR
Genes defining epithelial-mesenchymal transition...
Focal adhesion
Elevated in HGSOC
Retinoblastoma gene in cancer
Genes encoding cell cycle related targets of E2F transcription factors
Genes involved in the G2/M checkpoint...
Cell Cycle, Mitotic
Cell Cycle
Enrichment (k/K)
p-value
3e-57
5.7e-10
1.1e-09
1.7e-09
D
Discovery
Validation
MUC16 abundance, log2FC
Collection:
HGSOC
LGSOC

Figure 4

A

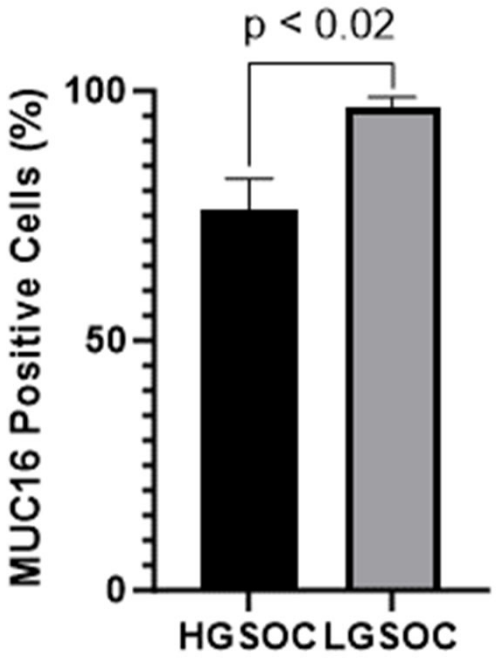
p < 0.02
MUC16 Positive Cells (%)
100
50
0
HGSOC
LGSOC

B

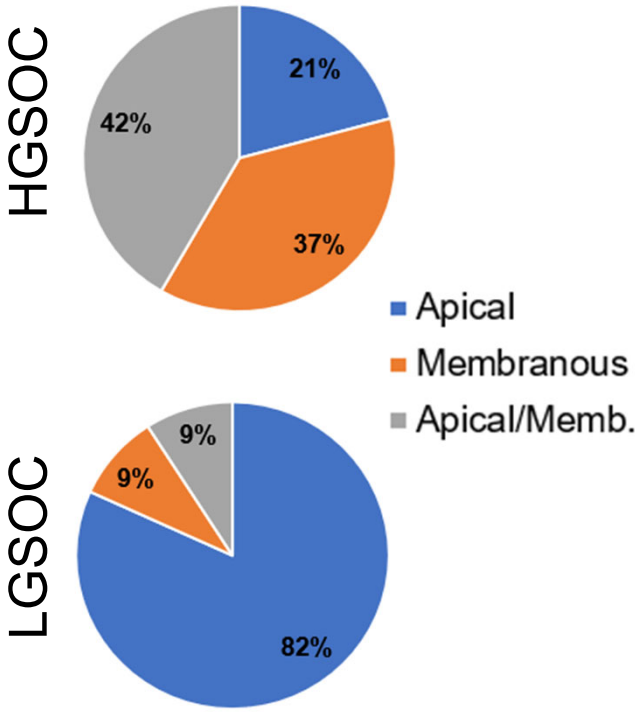
HGSOC
21%
37%
42%
LGSOC
9%
9%
82%
Apical
Membranous
Apical/Memb.

C

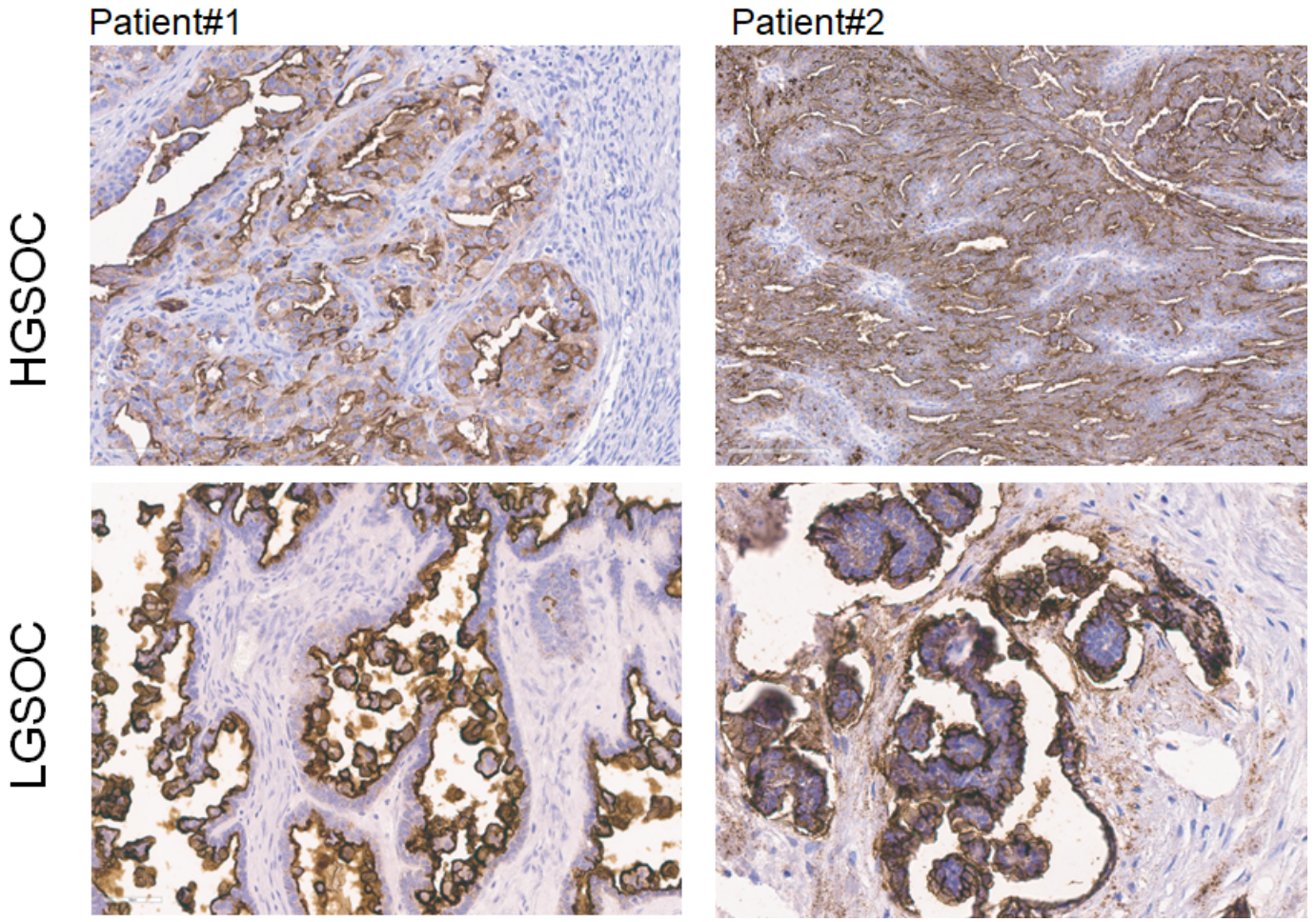
Patient#1
Patient#2
HGSOC
LGSOC